ACS APPLIED MATERIALS & INTERFACES

Forum Article

www.acsami.org

Binary and Bidisperse Polymer Brushes: Coexisting Surface States

Dirk Romeis*[,†] and Jens-Uwe Sommer[†,‡]

[†]Leibniz-Institut fuer Polymerforschung Dresden e.V., Hohe Strasse 6, 01069 Dresden, Germany

[‡]Institut fuer Theoretische Physik, Technische Universitaet Dresden, 01069 Dresden, Germany

ABSTRACT: In the present work, we consider polydispersity effects on a mixed polymer brush. Two types of polymer chains with different solvent selectivity being densely grafted together onto an impenetrable surface are forming a binary mixed polymer brush. Using a numerical quasi off-lattice self-consistent field method for heterogeneous chains we study the brush profile upon varying the strength of solvent selectivity (e.g., temperature) and the degree of polymerization of the two chain types (N_1 and N_2, respectively). For a monodisperse brush ($N_1 = N_2$) it is well-known, that the two types of polymers segregate into a two-layer structure, if the difference in solvent selectivity is increased. The state where the chains exposed to their good solvent forming the top layer of the brush can be frustrated for shorter chains and an inversion of the layering takes place. In the inverted state, the top layer is formed by long chains exposed to poor solvent covering the layer of shorter chains. By varying the solvent selectivity of the long chains we show that coexistence of the two states occurs,which indicates a discontinuous phase transition scenario for the switching process. We consider further the case of a very low fraction of short chains and find these chains to undergo a conformational transition of first order from a "coil" state, found deep inside the compact brush layer, to a "flower" state, stretching to the top of the brush upon varying the strength of the solvent selectivity. At the transition both states are found to be quasi-stable with an energy barrier of the order of the chain length in units of k_BT. The discontinuous nature of the switching process by combining solvent selectivity and bidispersity can be of high interest for the creation of stimuli-responsive surfaces.

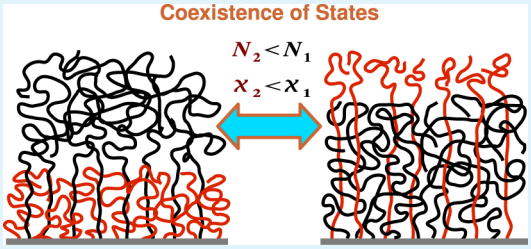

KEYWORDS: *Mixed Polymer Brush, Self-Consistent Field, Surface Instability, Conformational Switching, Smart Surface Coating, Stimuli-Responsive Material*

1. MOTIVATION

A polymer brush is formed by densely grafting the chain ends of polymers onto a surface. This tethering of the long macromolecules has considerable influence on the surface properties.[1] Upon changing the environmental conditions, e.g., temperature, pH, salt concentration, or light induction, the polymers and thereby the surface properties can be strongly modified.[2−8] In this context, it is of special interest to understand and control the behavior of the grafted layer and to create surfaces that display a desired response to external stimulation.

In a previous wor,k[9] we studied the case of a planar polymer brush with a fraction of free chain ends being replaced by a modified end-group, differing in size and solvent selectivity. Upon changing the solvent conditions, a switching in location of end-groups that are bigger than monomers could be observed and proved to be in agreement to molecular dynamics simulations (MD).[10] Such a system displays a stimuli-responsive behavior as surface properties (e.g., the end-groups pass from a state exposed to the solvent, on the top of the brush, to a hidden state, inside the brush) can be controlled by changing certain external conditions (here: solvent selectivity of the end-groups).

Another well-known implementation of smart surface coatings often denoted in literature are mixed or binary brushes, which are composed of two chemically distinct types of chains. First theoretical and simulation studies appeared around 20 years ago.[11,12] Experimental realizations and applications can be found elsewhere[13−16] and references therein. In dependence of solvent conditions and the composition of the polymer chains the two chain types phase separate into a bottom layer, at the grafting surface, and a top layer forming the brush surface. In Figure 1, this layering of the polymer types at different solvent selectivity is shown.

Here, in the left picture, the "dark blue" chains demix from the solvent molecules and so forming a compact phase at the bottom. The 'light blue' polymers, favoring solvent-monomer mixing, stretch through that compact layer to reach the solvent phase. The pictures are taken from MD studies of mixed monodisperse brushes for comparable fractions of the two different chain types.[17,18] The authors report a dynamically fast and reversible switching process with both layers inverting their positions upon inverting the solvent selectivity (center and right picture in Figure 1).

In the present, work we apply our recently developed self-consistent field (SCF) method[9,19,20] to the case of a binary mixed brush and analyze the switching behavior in detail,

Special Issue: Forum on Polymeric Nanostructures: Recent Advances toward Applications

Received: November 14, 2014
Accepted: February 3, 2015
Published: February 27, 2015

DOI: 10.1021/am507959k
ACS Appl. Mater. Interfaces 2015, 7, 12496−12504

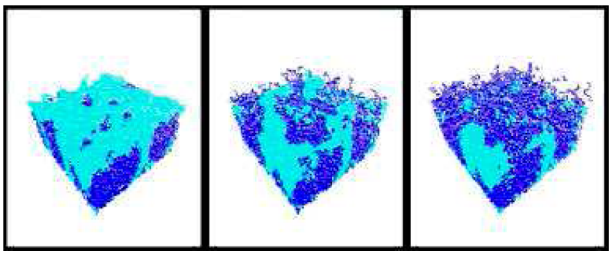

Figure 1. Snapshots from MD simulations of a mixed polymer brush. In the left picture, the "dark blue" polymers demix from the solvent and form the bottom layer, whereas the "light blue" chains favor solvent-monomer mixing and form the top layer. Then, the solvent selectivity is inverted and the layers rearrange (center and right picture). ($N_1 = N_2 = 128$, $\sigma = 0.116$).

especially with respect to a differing chain length (N_1 and N_2) for the two polymer types. Although the case of monodisperse mixed brushes ($N_1 = N_2$) has received considerable attention already, much less is known about polydispersity effects in these systems.

This work is structured as following. In section 2, we give a short introduction to properties of (mixed) polymer brushes. In section 3, we briefly sketch our numerical SCF approach. Using this method, we consider in section 4 the case of mixed polymer brushes for comparable fractions of both chain types, and in section 5, we assume only a small portion of brush chains being chemically different from the majority chains. In this limit, our approach proved to be very efficient. Finally, in section 6, we summarize the results and give our conclusions.

2. INTRODUCTION

We define the grafting density σ dimensionless in units of the size of a monomer b

$$\sigma = \frac{Mb^2}{A} \tag{1}$$

where M is the number of grafted chains and A the surface area. To form a polymer brus,h the grafting density must be larger than the overlap density $\sigma^* \approx b^2/R_{g_0}^2$ (with $R_{g_0}^2$ the radius of gyration of an isolated chain). In the following, we always consider the case $\sigma \gg \sigma^*$.

A first theoretical approach to describe polymer brushes was developed by Alexander and de Gennes,[21,22] recognizing the thickness of the grafted layer h_{brush} (brush height) to scale like

$$h_{\mathrm{brush}} \propto N\sigma^{(1-\nu)/2\nu} \tag{2}$$

where N denotes the chain length (number of chain segments) and the Flory exponent ν. Using the Flory estimate $\nu \simeq 3/5$ (good solvent conditions) one obtains $h_{\mathrm{brush}} \approx N\sigma^{1/3}$.

The important result here is that the chains in a polymer brush adopt strongly stretched conformations (e.g., radius of gyration $R_g \approx h_{\mathrm{brush}} \propto N$). Hence, universal features as originating from the "coil-like" conformations are not valid if the chains are densely grafted together. Especially, the equation of state and finite stretching of the molecules become relevant,[23−26] leading to a more steplike brush profile in comparison to previously calculated parabolic form based on Gaussian chains.[27,28] It has been shown in previous works that profiles having a strong gradient in the surface region lead to instabilities with respect to a change in chain length and shape of the end-groups.[9,10,19,20,29,30]

2.1. Mixed Polymer Brushes. If two types of chains are densely grafted together, they form a mixed brush. A typical example might be a considerable chain length difference ($N_1 \neq N_2$). Evidently, and as it is also well-known,[19,31−34] the longer chains stretch further away from the grafting surface, forming a layer at the top of the brush. Another mixed system is the case where a fraction of chains consists of monomers being chemically different from the other brush chains. The important feature here is the difference in the behavior with respect to the solvent molecules. In the following we assume that the environment is characterized by its hydrophobicity and we denote one type of chains (or monomers) as hydrophilic and the other type as hydrophobic chains/monomers. Such a mixture of hydrophilic and hydrophobic polymers grafted onto a substrate form a so-called binary brush.[35] For comparable fractions of the two chain types, binary brushes have been considered widely in the literature using various techniques, theoretical and experimental.[13,16−18,35,36] It is known that the system tends to phase separate (microphase separation) with the hydrophobic chains forming a bottom layer in aqueous environments (they adopt less stretched conformations and form a compact layer to reduce the contact area with the solvent molecules). The hydrophilic chains then have to stretch through the hydrophobic layer to be exposed to the good solvent and they form the top layer. In Figure 1, we display snapshots from molecular dynamics simulation carried out in our group for monodisperse binary mixed brushes showing the switching behavior under a change of the solvent conditions. This can be achieved by successively replacing the solvent by another, varying the pH or changing the temperature in such a way that the solvent conditions for both chain types are inverted and the two chain types rearrange[13,17,18] (see Figure 1). The authors[17] report a dynamically fast and reversible switching process.

2.2. Conformational Transitions and Polymer Brushes. It has been identified that the neighboring chains in a polymer brush impose a very special environment on a grafted chain itself.[37−39] Small changes in the brush profile, actually of $O(N^{-1})$,[37] are sufficient to find chain conformations in substantially different states. The special feature of the chain conformations in polymer brushes can be understood from the fact, that endmonomers are found over the whole brush height[26−28] and therefore fluctuations of the endmonomers height position z_e scale with the contour length of the whole chain: $\langle \Delta z_e \rangle \approx h_{\mathrm{brush}} \propto N$.

Mutually, this finding reveals a remarkable property of chain conformations in polymer brushes, constituted of sufficiently long chains: Any slight variation in the interaction of a grafted chain with the other brush chains has an enormous impact on the endmonomer position $g_e(\mathbf{r})$, especially in densely grafted brushes with a boxlike density profile.[9,10,19,20,29,30]

A possible implementation of this effect is the consideration of mixed polymer brushes containing chains that differ in some way from each other. In previous works, we suggested and analyzed certain modifications of a fraction of brush chains.[9,19,20,30] We found a conformational transition of the modified chains from a hidden state, deep inside the brush profile, to an exposed state, where its free chain end is located on top of the brush surface. The transition is most pronounced for strongly stretched brushes where the finite extensibility of chains plays a role. Because slight modifications of grafted chains have huge effects on their conformations inside the brush it is necessary to carefully take into account an adequate

DOI: 10.1021/am507959k
ACS Appl. Mater. Interfaces 2015, 7, 12496−12504

description of the chain model and the interactions. In addition, to analyze a conformational phase transition we need to regard conformational fluctuations.

In this work, we will study the combination of the two effects: solvent selectivity and instability with respect to chain length variation. We will show that this leads to first-order-like switching scenario where the coexistence of two states is expected.

3. THE SELF-CONSISTENT FIELD METHOD

In previous work[9,19,20] we presented a quasi off-lattice numerical SCF approach for freely jointed polymer chains of spherical segments of variable sizes and solvent selectivity. It could be shown that the results of this method for monodisperse homopolymer brushes are in quantitative agreement with MD simulation[10,29] results without any parametrization or fitting of the data. It accounts for conformational fluctuation, depletion and packing effects. Additionally, we could prove[30] that the approach is in very good agreement with other methods to describe the conformational transition in a brush. In the following, we shortly sketch our method. For details, see refs 9, 19, and 20.

The SCF scheme is a mean-field method approximating the actual many chain problem by a "single" chain problem in an unknown external field $V_i(\mathbf{r})$ (index i for different chain types). For a given $V_i(\mathbf{r})$, the local occupation density $\phi_i(\mathbf{r})$ is obtained

$$\varphi_i(\mathbf{r}) = \mathcal{F}[V_i(\mathbf{r})] \tag{3}$$

The field $V_i(\mathbf{r})$ accumulates all interactions, that a monomer/particle experiences, into one function describing, e.g., overlapping, attraction, and repulsion. This field itself results from the average local occupation densities $\phi_i(\mathbf{r})$ and represents the local chemical potential

$$V_i(\mathbf{r}) = \mu_i(\{\varphi_j(\mathbf{r})\}) \tag{4}$$

where $\mu_i(\{\phi_j(\mathbf{r})\})$ denotes the equation of state for the system under consideration. The crucial point in SCF is to chose an accurate equation of state and to calculate eqs 3 and 4 self-consistently.

The present approach[9,19,20] is a one-dimensional reduced description of a polymer brush model, where we only take into account the height profile (z-coordinate) and in lateral directions (x, y) the brush is assumed to be homogeneous. Previous studies suggest that hydrophobic layers adopt different three-dimensional morphologies, e.g., "ripples" (stripelike), "dimples" (droplike),[40,41] or micelles.[42] Such lateral ordering phenomena and their effect on the height profile in binary brushes are neglected in a 1D approach. Recent detailed investigations on polymer brushes in poor solvent revealed an increasingly flat phase boundary between the solvent rich and the polymer rich phase at the brush surface for increasing grafting densities.[43] This is the regime of interest for a mean-field description of polymer brushes.[44,45]

To consider arbitrarily shaped chain segments we introduce a discretization scheme below the length of a "segment". Our approach is sketched in Figure 2. The number of sites of the "sublattice" is denoted D_s. With larger D_s we more and more approach the continuous limit.

The diameter of any sphere of type i (any segment or nanoparticle of another sort or size) is denoted as λ_i. Assume the center of some sphere of type i being located at position z, then the center of a sphere of type j connected to the previous

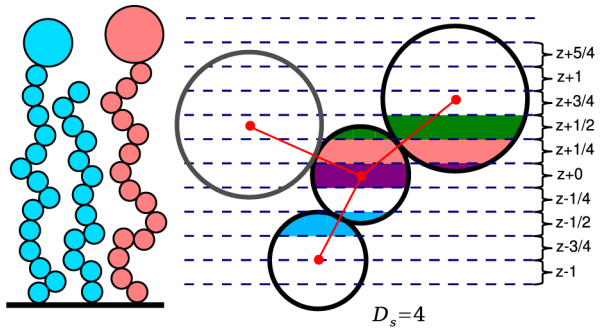

Figure 2. Sketch of the method. Left: Chains of heterogeneous spherical segments. Right: Example for connected spheres on a "sublattice" with $D_s = 4$.

one can be located at the sites $z' = z + d_s/D_s$, with $|d_s| \in [0,D_s(\lambda_i+\lambda_j)/2]$. In Figure 2 some possible positions of connected spheres are sketched. The probabilities $w_{i,j}$ are given by the relative angle range Ω_{d_s} covering the corresponding site

$$w_{i,j}(d_s) = \frac{1}{4\pi}\int_{\Omega_{d_s}} d\Omega \tag{5}$$

With these $w_{i,j}(d_s)$, we introduce a recurrence relation for the partition function $G_K(n, z_0, z)$ of a chain of type K having its first segment located at z_0 and the $(n + 1)$th segment at z that reads

$$G_K(n+1, z_0, z) = e^{-V_{n+1}(z)}\left\{\sum_{d_s=-D_s}^{D_s} w_{n,n+1} G_K\left(n, z_0, z + \frac{d_s}{D_s}\right)\right\} \tag{6}$$

with the initial condition $G_K(0, z_0, z) = \delta_{z0,z}$. Here, $V_n(z)$ denotes the mean field potential acting on the sphere or segment n with its center of mass at site z. This way we also allow for different interactions for certain types of segments. This relation eq 6 describes the position of the centers of spheres that are connected to a chain of type K (certain sequence of different segments). The center of mass distribution of the different segments is calculated via[44]

$$\gamma_i(z) = \sum_K \sigma_K D_s \sum_{n=0,n\in i}^{N_K} \frac{G_K(n, z_K, z)\sum_{z'} G_K(N_K - n, z, z')}{\sum_{z'} G_K(N_K, z_K, z')} \tag{7}$$

Where N_K denotes the length of chain type K, σ_K its grafting density and z_K its grafting position (the grafted chain end). Accordingly to the spherical shape, the average volume occupation density $\phi_i(z)$ of the segments interacting with each other at some site z is obtained (see differently colored slices in Figure 2).

The self-consistency is provided via the equation of state. For the mean field description of the volumetric interactions of spheres the Boublik−Mansoori−Carnahan−Starling−Leland equation[46−48] proved to be a very accurate equation of state (EoS). The excess free energy of mixing of a multicomponent system is given as

DOI: 10.1021/am507959k
ACS Appl. Mater. Interfaces 2015, 7, 12496−12504

$$F_{\mathrm{mix}}^{\mathrm{BMCSL}} = \mathcal{N}\left\{\left(\frac{\zeta_2^3}{\zeta_0\zeta_3^2} - 1\right)\ln(1-\zeta_3) + \frac{3\zeta_1\zeta_2}{\zeta_0(1-\zeta_3)} + \frac{\zeta_2^3}{\zeta_0\zeta_3(1-\zeta_3)^2}\right\} \quad (8)$$

With

$$\zeta_\alpha = \frac{\pi}{6}\sum_i \frac{\mathcal{N}_i}{V}\lambda_i^{\alpha} = \sum_i \varphi_i \lambda_i^{\alpha-3} \quad (9)$$

The total number of particles is defined as $\mathcal{N} = \sum_i \mathcal{N}_i$ and we have $\mathcal{N}_i$ spheres of a certain type i. Because in a polymer chain the segments are connected to one another, we have to add a correction term that accounts for the connectivity of the spheres. We choose the proposition made previously[26,49] and omit the term $-k_B T \mathcal{N}_i \ln(1-z_3)$ (translational entropy) in eq 8. To model additional short-range attraction between certain types of segments we introduce a Flory–Huggins $\chi_{i,j}$-parameter in the second order term of the virial expansion of the free energy. This is a very common description in mean field theories. We will define the additional term in the following way

$$\frac{F_{\mathrm{attr}}}{V} = -\frac{36}{\pi}\sum_{i,j}\chi_{i,j}\varphi_i\varphi_j \quad (10)$$

The $\chi_{i,j}$ parameters fix the cross interactions between particles of type i and j and must be symmetric. Note, for attraction the χ parameters are defined positive and are rescaled such, that the second virial in the total free energy of a homopolymer solution becomes zero for $\chi = 0.5$ and the leading order for volumetric interactions is of third order, consistent with the definition of the Θ-point in a polymer solution.[50] For $\chi > 0.5$, the second virial becomes negative and we enter the regime of poor solvent conditions. The final form of the EoS we use in our approach is discussed in the appendix of a previous work.[9]

With respect to an implicit aqueous solvent we define a model for a binary brush as follows: One class of monomers (type 1) which we call hydrophobic is defined by a $\chi_{1,1} > 0$. The other class (type 2) is defined by a constant $\chi_{2,2} = 0$ and these monomers are denoted hydrophilic. For the interactions between chain monomers of different types we set $\chi_{1,2} = 0$ (they are purely repulsive). These choices are analogue to the system studied via MD simulations.[17] For simplicity, we will denote the difference in solvent selectivity by χ: = $\chi_{1,1}$.

4. COMPARABLE FRACTION OF VARIOUS CHAINS IN MIXED BRUSHES

4.1. Monodisperse Brushes. In the following we denote the relative fractions of different chain types in a mixed brush by f_i (e.g., $f_1 = 1 - f_2$) and the total grafting density by σ.

In Figure 3 the density profiles (in z-direction, perpendicular to the wall) of a binary brush as obtained via MD simulation[17] are displayed. Using implicit solvent the solvent selectivity is modeled via a Lenard-Jones potential with changing cutoff parameter ϵ.

In Figure 4 the SCF calculations for the density profiles (top) and endmonomer distributions (bottom) for varying χ are shown. The grafting density, the chain length and the relative fraction of both chain types are identical to those presented in Figure 3. Comparing the upper panel in Figure 4 as well as

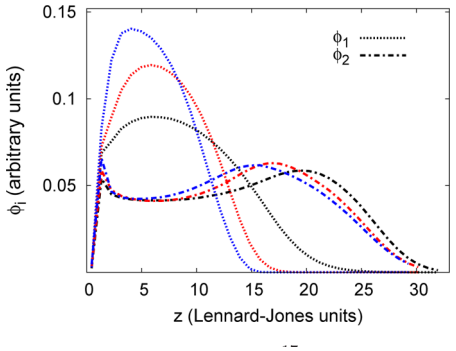

Figure 3. Simulation results[17] for a binary polymer brush. Volume density (ϕ_1 and ϕ_2) for both chain types. Different colors indicate different solvent selectivity for chain type 1. ($\sigma = 0.116$, $N_1 = N_2 = 64$, $f_1 = 50\%$).

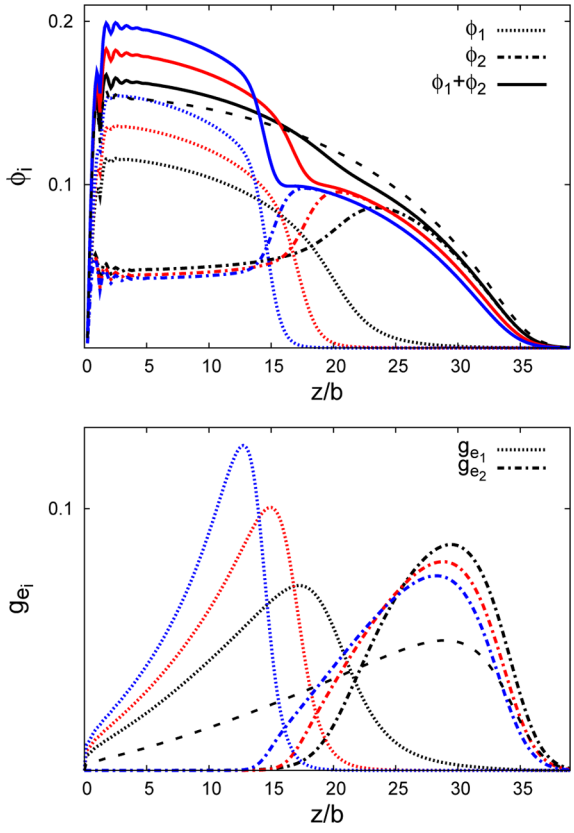

Figure 4. Results of SCF calculations of a binary mixed polymer brush for various solvent selectivity: $\chi = 0.2$ (black), $\chi = 0.4$ (red), $\chi = 0.7$ (blue). Top: density profiles. Bottom: endmonomer distributions. ($\sigma = 0.116$, $N_1 = N_2 = 64$, $f_1 = 50\%$, $D_s = 8$). In addition are shown the calculations for a corresponding athermal homopolymer brush (black dashed curves).

Figure 3 the similarity is striking. The parameter ϵ (varying cutoff) in Figure 3 and the change in the second virial coefficient in our mean-field description can not be directly mapped to each other, but a qualitative correspondence between χ in Figure 4 and ϵ in Figure 3 can be drawn by considering the Θ-point for a homogeneous solution of polymer chains ($\chi = 0.5$ in our method, see eq 4[17]). The black curves in Figure 3 and Figure 4 are still well below Θ conditions. Both chain types are beginning to phase-separate, but no marked interface has evolved. The overall density profile

DOI: 10.1021/am507959k
ACS Appl. Mater. Interfaces 2015, 7, 12496–12504

(ϕ_1 + ϕ_2) is very similar to the corresponding athermal homopolymer brush (dashed line). Around the Θ-point (red curves) the phase separation is enhanced and above Θ conditions (blue curves) the hydrophobic chains form a compact layer at the grafting surface and a marked interface (around z = 15 b) has evolved. Nevertheless, an increasing solvent selectivity has almost no influence on the overall height of the binary brush. This is confirmed by the MD simulations.

In the bottom of Figure 4 the corresponding endmonomer distributions g_e are plotted. The free ends of both chain types clearly localize in different height positions. No hydrophilic endmonomers are found in the bottom layer close to the grafting surface. With increasing χ the hydrophobic chain ends localize closer to the grafting surface, whereas the hydrophilic chain end distributions remain very similar upon varying χ. That the hydrophilic layer is not much influenced by a change of the solvent conditions is also found via MD simulations.[17]

4.2. Varying the Chain Length: Multiple SCF Solutions. In the following we consider binary brushes in a hydrophilic environment, where the hydrophilic chains are shorter than the hydrophobic ones. This will frustrate the enthalpically preferred state where the hydrophilic chains are exposed to the good solvent. Hence, we face a diametrical interplay between chain length difference and solvent selectivity.

In Figure 5 the density profiles for a certain parameter set are shown. As expected,[31,33] in case of a nonselective solvent (χ = 0) the shorter chains (ϕ_2 with N_2 = 44) form the first layer near the grafting surface and the longer chains (ϕ_1 with N_1 = 64) stretch through that layer and segregate on the top. For highly selective solvent (χ = 2.0) the layers have been inverted and the phase separation is very pronounced. The long hydrophobic chains form a very dense and compact layer at the grafting surface and the short hydrophilic chains now strongly stretch through that layer in order to reach the solvent-rich phase. Note the range of oscillations in the profile of ϕ_1 and ϕ_2 for χ = 2.0 indicating that the monomers are packed densely.

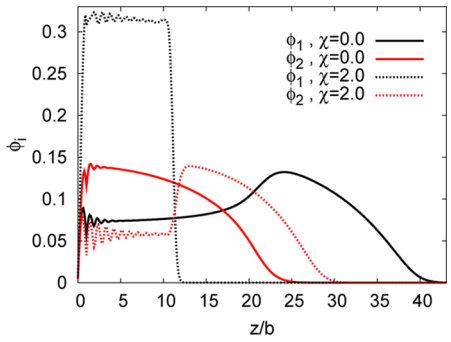

Figure 5. Composition profiles as obtained by SCF calculation of a mixed polymer brush (hydrophilic/hydrophobic chains) with different chain lengths (N_1 = 64, N_2 = 44, f_1 = 50%, σ = 0.2).

No matter what choice for χ was made: A mixed state could not be found. In contrast, for certain sets of parameters multiple solutions appeared. The remarkable observation in our study is that that multiple (coexisting) solutions for ϕ_1 and ϕ_2 could only be encountered if $N_1 \neq N_2$.

In Figure 6 the corresponding profiles for χ = 1.0 and χ = 1.5 are presented. The plot in the top of Figure 6 shows the case, where the long hydrophobic chains form the bottom layer and the shorter hydrophilic chains form the second layer on top.

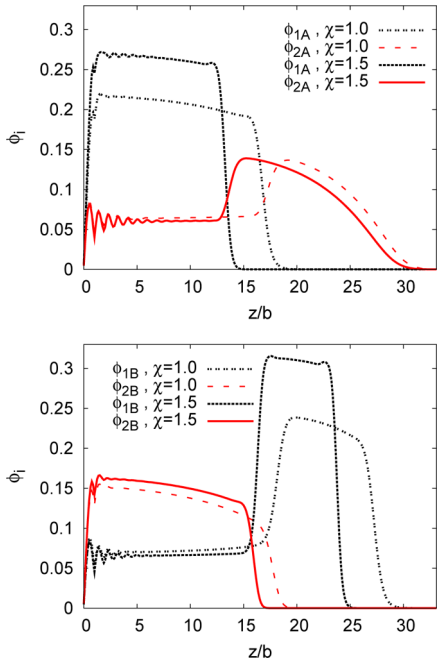

Figure 6. Composition profile of two self-consistent solutions for the same parameter set as in Figure 5. Top: Solution type A (sequence ϕ_1 ϕ_2). Bottom: Solution type B (sequence ϕ_2 ϕ_1). (σ = 0.2, f_1 = 50%, N_1 = 64, N_2 = 44, D_s = 8).

This type of layering we call 'A'. With increasing χ the hydrophobic layer becomes more and more compact and the overall brush height remains almost constant ($z \approx 30\ b$, compare also χ = 2.0 in Figure 5).

In the bottom of Figure 6 the other type of solutions, 'B', is presented. Here, the short hydrophilic chains form the bottom layer. They do not stretch through the compact hydrophobic layer formed on the top of the brush. With increasing χ, again, the hydrophobic layer, becomes more dense and compact. With compression of the hydrophobic layer the hydrophilic layer gets squeezed between the grafting surface and the compact top layer. Compared to χ = 0.0 in Figure 5 the hydrophilic layer has been compressed by around 30% for χ = 1.5. Since the effective interactions for the hydrophilic chains have been left unchanged this phenomena is remarkable as it is mediated solely by the change in the solvent quality experienced by the hydrophobic chains. With increasing χ the top layer aims to adsorb more and more hydrophobic monomers, but due to the grafting condition the hydrophilic chains have to be compressed in order to increase the amount of hydrophobic material in the top layer. Note that layering type 'B' builds up two phase boundaries and the overall brush height is noticeably reduced (compare also χ = 0.0 in Figure 5).

Starting from a bidisperse brush in nonselective solvent the short chains (N_2) always form the bottom layer (their chain ends are never found at the brush surface). With increasing selectivity the monomers of the longer N_1-chains in the top layer crowd together and build up a cover of increasing density. This cover, on the other hand, additionally handicaps the hydrophilic N_2-chains to reach the top of the brush (solution type 'B' in Figure 6 and Figure 7). The pressure acting on the two layers is increasing. At some point this pressure is so high that the system fully inverts the two layers (solution type 'A' in Figure 6 and Figure 7). For very large χ only profiles of type 'A' can be obtained just as for low χ only type 'B' is retrieved as the

DOI: 10.1021/am507959k
ACS Appl. Mater. Interfaces 2015, 7, 12496−12504

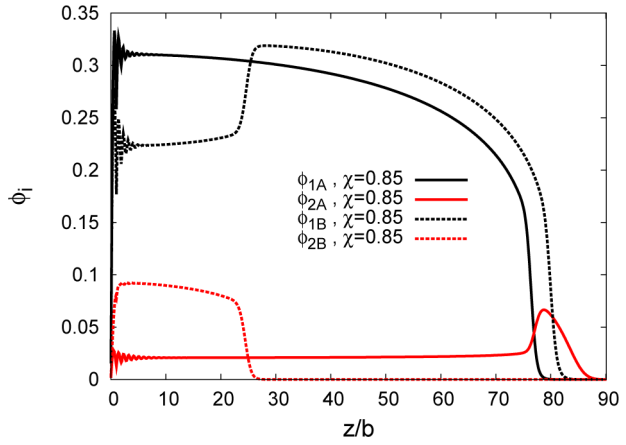

Figure 7. Coexisting SCF solutions for another parameter set: N_1 = 128, N_2 = 112, f_1 = 90%, σ = 0.35.

self-consistent solution. At intermediate χ both states are possible. They are metastable, and the lower and upper bounds of χ, where multiple solutions are found mark the spinodal lines of a first order phase transition. In Figure 7 are shown the corresponding two solution types for a different set of parameters where in particular the fraction of short hydrophilic chains is low.

We state the following result: For a given chain length difference there exists a range in χ where both types of layering may coexist.

From the well-known behavior of bidisperse homopolymer brushes,[19,31−34] as well as that of monodisperse binary (mixed) brushes,[17,18] which could be confirmed by our SCF method in section 4.1, and the results presented here we draw a qualitative phase diagram for the general case of bidisperse and binary brushes in Figure 8. Comparing the results for several

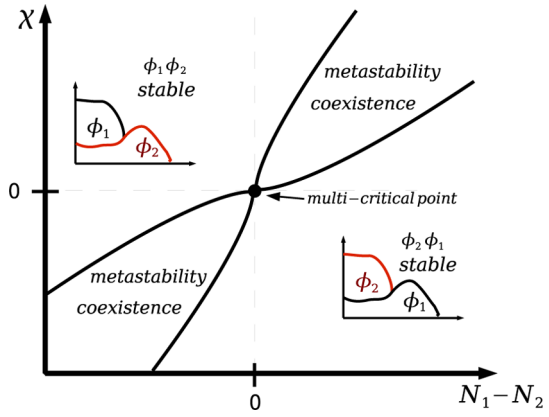

Figure 8. Qualitative sketch of the phase diagram of a binary (difference in solvent selectivity $\chi = \chi_{1,1} - \chi_{2,2}$) and bidisperse (chain length N_1 respectively N_2) polymer brush.

parameter sets we also found that with increasing chain length difference $N_2 - N_1$ the range $\Delta\chi$, where two metastable states coexist and a discontinuous phase transition is predicted, increases as well. With $N_2 \rightarrow N_1$ one reaches a critical point, where no coexisting states can be found. Also in the case of bidisperse homopolymer (χ = 0) brushes we have only one unique solution, where the shorter chains always form the bottom layer. Therefore, we denote this point a multicritical point.

5. VERY LOW FRACTION OF HYDROPHILIC GUEST CHAINS

In order to investigate the conformational transition of hydrophilic chains in an environment of hydrophobic chains of different length in more detail, we consider individual modified guest chains grafted additionally into a homopolymer brush. In this limit $f_2 \rightarrow 0$ we can analyze the partition function of a single test chain in the presence of the self-consistent profile of the homopolymer brush. We note that in the limit $f_2 \rightarrow 0$ we no longer have to deal with coexisting solutions.

To distinguish between the binary brushes with finite values f_2 discussed in the previous section we introduce the following notation: The majority brush chains are of given length $N_1 = N$, which are exposed to varying solvent conditions (controlled via the χ parameter) and a test chain of varying length $N_2 = N^*$ interacting strictly under athermal solvent conditions. This test chain method has been introduced in our previous work.[9,19,30] The conformational transitions of minority chains in a polymer brush have been studied via different approaches recently.[51]

In Figure 9 we display the endmonomer distributions, g_e^*, of the hydrophilic test chain. For $\chi \approx 1.3$ the endmonomer

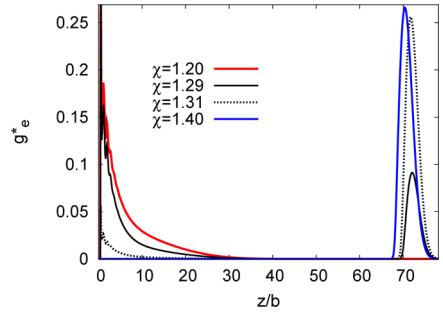

Figure 9. Endmonomer distributions $g_e^*(z)$ for hydrophilic test chains upon varying solvent quality for majority brush chains. (N = 128, N^* = 91, σ = 0.35).

distributions display two very sharp maxima at the grafting surface and on the top of the brush. At lower χ values the end of the hydrophilic chain is strictly found at the grafting surface, whereas for larger χ it is localized on top of the brush, but it is never found at intermediate positions (e.g., 30 $b < z <$ 65 b). At very low fractions of hydrophilic chains in a hydrophobic majority brush we thus encounter a first-order coil-to-flower transition.[52]

In Figure 10 the free energy landscape F_{N^*} for the position z_e^* of the chain end is displayed for various χ values. The brush

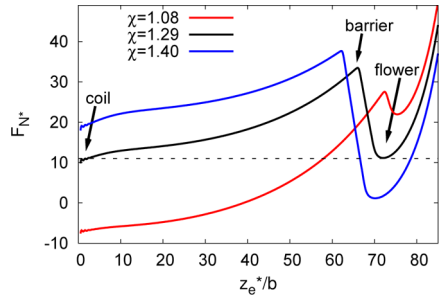

Figure 10. Free energy landscape in units of k_BT in dependence of the height position z_e^* of a hydrophilic chain with N^* = 91 for different χ values at σ = 0.35 and N = 128.

DOI: 10.1021/am507959k
ACS Appl. Mater. Interfaces 2015, 7, 12496−12504

parameters are the same as for the chain end distributions g_e^* in Figure 9. There, two pronounced maxima in g_e^* were encountered within a quite narrow range of χ ($\Delta\chi \approx 0.03$). The free energy landscape in Figure 10 displays coexisting minima (corresponding to "coil" and "flower") for a much broader range. For $\chi = 1.4$ the probability to find the test chain in the "coil" state (close to the grafting surface) in comparison to the 'flower' state is almost zero ($O(e^{-20})$), but nevertheless, the local minimum for the 'coil' state remains. If for this parameter set the test chain is somehow prepared in the 'coil' state it has to overcome a large energy barrier ($\Delta F_{N^*} \approx 15 k_B T$) to switch to the (energetically favored) "flower" state. This proves the large range of metastability with quasi-stable coexisting states for the test chains.[52]

In Figure 11 the endmonomer distributions at low solvent selectivity and variable test chain length are plotted. Indeed, the

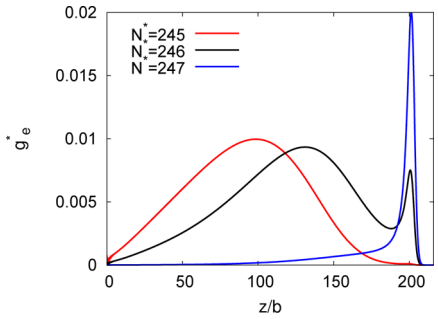

Figure 11. Endmonomer distributions $g_e^*(z)$ for hydrophilic test chains of different chain lengths N^* at low solvent selectivity $\chi = 0.25$ (N 256, $\sigma = 0.45$).

first-order character of the conformational transition is already emerging for any $\chi > 0$ and $N^* < N$. This is contrast to the case $\chi = 0$ and $N^* \neq N$,[19,30] where a continuous transition from the "coil" to the "flower" state was found. That such small variations in the solvent selectivity has such drastic effects is remarkable and reveals once again the very sensitive behavior of chain conformations in dense polymer brushes.

In Figure 12 the average height position $\langle z_e^* \rangle / N$ of the hydrophilic chain end is plotted versus the χ-parameter for

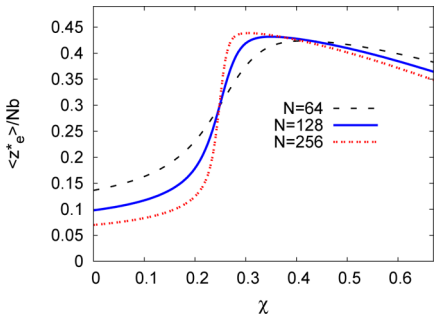

Figure 12. Average height position $\langle z_e^* \rangle$ of the endmonomer of the test chain upon varying solvent selectivity χ ($n^* = (N - N^*)/N = 0.14$, $\sigma = 0.1$).

different N at constant relative chain length difference $n^* = (N - N^*)/N$. The transition point is independent of N, but the transition itself sharpens toward a step-function for longer brush chains N. Hence, brushes of very long chains display a more sensitive switching for the case of a switchable minority component, whereas the transition point itself is not altered.

In order to further analyze the switching behavior in dependence of majority brush parameters we define a critical condition for the transition between the two states by the inflection point of the height of the hydrophilic chain end with respect to the solvent selectivity:[9]

$$S = \left. \frac{|\Delta\langle z_e^* \rangle|}{\Delta\chi} \right|_{\chi_{crit}} \rightarrow \text{Max} \tag{11}$$

The value χ_{crit} is defined the transition point, where the change in the average height position $\Delta\langle z_e^* \rangle / N$ upon varying the χ-parameter becomes a maximum. The value of S itself indicates the sensitivity of the transition.

In Figure 13 the results for χ_{crit} obtained within the numerical SCF method are plotted versus n^*. The discretization step for χ

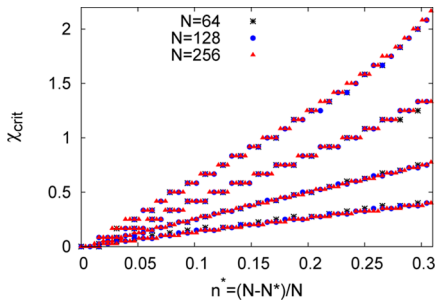

Figure 13. Critical χ parameter in dependence of relative chain length difference $(N^* - N)/N$ and grafting density. In ascending order: $\sigma = 0.05$, $\sigma = 0.2$, $\sigma = 0.35$, and $\sigma = 0.45$).

was chosen as $\Delta\chi = 0.025$ ($\sigma = 0.05$ and $\sigma = 0.2$), respectively $\Delta\chi = 0.0825$ ($\sigma = 0.35$ $\sigma = 0.45$). The universality with respect to the length of the majority brush chains is well observed. For a given σ the data points fall on a single straight line. Hence, the critical parameter, where the coil-to-flower transition occurs, is linearly proportional to n^* (relative chain length difference). The slope of the lines is increasing the larger the grafting density of the brush is.

If the hydrophilic chain length is further decreasing the linear relation is lost and χ_{crit} adopts increasing larger values. For $\sigma = 0.45$ the data points above $n^* \approx 0.25$ leave the straight line. The breakdown of this linear scaling is also observed for very short N^* chains (large n^*) at lower grafting densities. Since our SCF approach considers finite extensible chains this deviation is expected: For short chains χ_{crit} diverges if $N^*b = h_{brush}$, the brush height equals their contour length. Then, the short chains have no possibility to reach the top of the brush. With increasing σ also the brush height increases (at fixed N) and hence finite extensibility comes into play at lower ratios n^*.

6. SUMMARY

For various types of brush systems the accuracy of the quasi off-lattice numerical SCF method has been tested in comparison to other methods.[9,19,20,30] Also in case of monodisperse binary brushes of comparable fractions of hydrophilic and hydrophobic chains we could show that the averaged height profiles as obtained from our SCF approach are in good agreement with corresponding MD simulation.[17] With increasing solvent selectivity χ the brush phase-separates with the hydrophobic

DOI: 10.1021/am507959k
ACS Appl. Mater. Interfaces 2015, 7, 12496−12504

chains forming the bottom layer and the hydrophilic chains stretching through that layer and form a swollen brush on top.

We then considered the case of bidisperse binary brushes in hydrophilic environment, where the short chain fraction is constituted by hydrophilic chains and the long chains being tunable hydrophobic. At low solvent selectivity of the long chains we find the short hydrophilic chains forming the bottom layer. If χ (strength of hydrophobic interaction of long chains) is very large both layers switch their position with the long hydrophobic chains forming now the bottom layer. At intermediate χ we find multiple solutions for the brush profiles within our SCF method. The coexistence of two different self-consistent solutions in a wide range of χ indicates a discontinuous (first order) transition between the two states. Coexisting states can only be found if the two chain types are of different length $N_1 \neq N_2$. The coexistence of the two conformational states of the brush indicates a first order transition involving metastable states in certain range of selectivity. These results can be used to define a phase diagram for the binary brush in the parameter space of chain length difference and solvent selectivity.

In order to investigate conformational transitions of individual hydrophilic chains grafted occasionally into a densely grafted brush constituted by a majority of hydrophobic chains we considered the case of a single hydrophilic test chain exposed to the self-consistent density profile generated by a hydrophobic brush. Within this test chain method the SCF profiles are unique and for a given chain length difference ($N^* \neq N$) we encounter a range χ where two pronounced maxima in the chain end distribution g_e^* of the test chain emerge.

Using the test chain method we found a large range χ of metastability for the coexistence of the "coil" and the "flower" state with a large free energy barrier separating the two states from each other. The conformational transition itself becomes more pronounced if the chain length of the hydrophobic brush chains and/or the grafting density σ is increased.

The point, where the conformational transition of the test chain occurs (critical solvent selectivity χ_{crit}) scales linearly with the relative chain length difference n^* until finite extensibility becomes important. The free energy difference between the two meta stable states can be as high as several 10 k_BT.

The method used here cannot account for lateral structure formation. Therefore, one might ask wether a coexistence of the two encountered states is a possible scenario in nature. It would be of principle interest to investigate in more detail the possibility to obtain a discontinuous phase transition for binary and bidisperse polymer brushes. The encountered phenomena of various coexisting profiles, which differ such remarkably from each other and that are found simultaneously stable within a large range of interaction parameters is worth to be studied using dynamical 3-D methods which take into account more of the relevant effects. Here, also pattern formation in the coexistence region might be expected. For coexisting states with a strong barrier in between "writing" and "erasing" of patterns by external stimuli could be a potential application.

AUTHOR INFORMATION

Corresponding Author

*E-mail: romeis@ipfdd.de.

Notes

The authors declare no competing financial interest.

ACKNOWLEDGMENTS

We thank H. Merlitz for fruitful discussions and providing the molecular dynamics simulation data. We are grateful to the DPG priority program SPP 1369 for financial support.

REFERENCES

(1) Currie, E.; Norde, W.; Stuart, M. Tethered Polymer Chains: Surface Chemistry and their Impact on Colloidal and Surface Properties. *Adv. Colloid Interface Sci.* **2003**, *100*, 205−265.

(2) Galuschko, A.; Spirin, L.; Kreer, T.; Johner, A.; Pastorino, C.; Wittmer, J.; Baschnagel, J. Frictional Forces between Strongly Compressed, Nonentangled Polymer Brushes: Molecular Dynamics Simulations and Scaling Theory. *Langmuir* **2010**, *26*, 6418.

(3) Spirin, L.; Galuschko, A.; Kreer, T.; Johner, A.; Baschnagel, J.; Binder, K. Polymer-brush Lubrication in the Limit of Strong Compression. *Eur. Phys. J. E: Soft Matter Biol. Phys.* **2010**, *33*, 307.

(4) Gupta, S.; Agrawal, M.; Uhlmann, P.; Simon, F.; Oertel, U.; Stamm, M. Gold Nanoparticles Immobilized on Stimuli Responsive Polymer Brushes as Nanosensors. *Macromolecules* **2008**, *41*, 8152−8158.

(5) Rosario, R.; Gust, D.; Hayes, M.; Jahnke, F.; Springer, J.; Garcia, A. Photon-Modulated Wettability Changes on Spiropyran-Coated Surfaces. *Langmuir* **2002**, *18*, 8062−8069.

(6) Russell, T. Surface-Responsive Materials. *Science* **2002**, *297*, 964−967.

(7) Lahann, J.; Mitragotri, S.; Tran, T.-N.; Kaido, H.; Sundaram, J.; Choi, I.; Hoffer, S.; Somorjai, G.; Langer, R. A Reversibly Switching Surface. *Science* **2003**, *299*, 371−374.

(8) Yoshida, R.; Sakai, K.; Okano, T.; Sakurai, Y.; Bae, Y.; Kim, S. Surface-Modulated Skin Layers of Thermal Responsive Hydrogels as on-off switches: 1. Drug Release. *J. Biomater. Sci., Polym. Ed.* **1991**, *3*, 155−162.

(9) Romeis, D.; Sommer, J.-U. Conformational Switching of Modified Guest Chains in Polymer Brushes. *J. Chem. Phys.* **2013**, *139*, 044910.

(10) Merlitz, H.; He, G.-L.; Wu, C.-X.; Sommer, J.-U. Nanoscale Brushes: How to Build a Smart Surface Coating. *Phys. Rev. Lett.* **2009**, *102*, 115702.

(11) Witten, T.; Milner, S. Two-Component Grafted Polymer Layers. *Mater. Res. Soc. Symp. Proc.* **1990**, *177*, 37−45.

(12) Lai, P.-Y. Binary Mixture of Grafted Polymer Chains: A Monte Carlo Simulation. *J. Chem. Phys.* **1994**, *100*, 3351−3357.

(13) Uhlmann, P.; Merlitz, H.; Sommer, J.-U.; Stamm, M. Polymer Brushes for Surface Tuning. *Macromol. Rapid Commun.* **2009**, *30*, 732−740.

(14) Bittrich, E. *Design of New Responsive Materials Based on Functional Polymer Brushes*; http://nbn-resolving.de/urn:nbn:de:bsz:14-qucosa-62669: Dresden, 2010.

(15) Uhlmann, P.; Houbenov, N.; Brenner, N.; Grundke, K.; Burkert, S.; Stamm, M. In-Situ Investigation of the Adsorption of Globular Model Proteins on Stimuli-Responsive Binary Polyelectrolyte Brushes. *Langmuir* **2006**, *23*, 57−64.

(16) Minko, S.; Luzinov, I.; Luchnikov, V.; Mueller, M.; Patil, S.; Stamm, M. Bidisperse Mixed Brushes: Synthesis and Study of Segregation in Selective Solvent. *Macromolecules* **2003**, *36*, 7268−7279.

(17) Merlitz, H.; He, G.-L.; Sommer, J.-U.; Wu, C.-X. Reversibly Switchable Polymer Brushes with Hydrophobic/Hydrophilic Behavior: A Langevin Dynamics Study. *Macromolecules* **2009**, *42*, 445.

(18) He, G.-L.; Merlitz, H.; Sommer, J.-U.; Wu, C.-X. Microphase Separation of Mixed Binary Polymer Brushes at Different Temperatures. *Macromolecules* **2009**, *42*, 7194.

(19) Romeis, D.; Merlitz, H.; Sommer, J.-U. A New Numerical Approach to Dense Polymer Brushes and Surface Instabilities. *J. Chem. Phys.* **2012**, *136*, 044903.

(20) Romeis, D. *Conformational Transitions in Polymer Brushes - A Self-Consistent Field Study*; http://nbn-resolving.de/urn:nbn:de:bsz:14-qucosa-139354, TU Dresden, 2014.

DOI: 10.1021/am507959k
ACS Appl. Mater. Interfaces 2015, 7, 12496−12504

(21) Alexander, S. Adsorption of chain molecules with a polar head - A scaling description. *J. Phys. (Paris)* **1977**, *38*, 983−987.
(22) de Gennes, P. G. Conformations of polymers attached to an interface. *Macromolecules* **1980**, *13*, 1069−1075.
(23) Shim, D.; Cates, M. Finite Extensibility and Density Saturation Effects in the Polymer Brush. *J. Phys. (Paris)* **1989**, *50*, 3535−3551.
(24) Lai, P.-Y.; Halperin, A. Polymer Brush at High Coverage. *Macromolecules* **1991**, *24*, 4981−4982.
(25) Amoskov, V.; Pryamitsyn, V. Theory of Monolayers of Non-Gaussian Polymer Chains grafted onto a Surface. *J. Chem. Soc. Faraday Trans.* **1994**, *90*, 889−893.
(26) Biesheuvel, P.; de Vos, W.; Amoskov, V. Semianalytical Continuum Model for Nondilute Neutral and Charged Brushes Including Finite Stretching. *Macromolecules* **2008**, *41*, 6254.
(27) Milner, S. T.; Witten, T. A.; Cates, M. E. Theory of the Grafted Polymer Brush. *Macromolecules* **1988**, *21*, 2610−2619.
(28) Zhulina, E. B.; Pryamitsyn, V. A.; Borisov, O. V. Structure and Conformational Transitions in Grafted Polymer Chain Layers. A New Theory. *Polym. Sci. U.S.S.R.* **1989**, *31*, 205−216.
(29) Merlitz, H.; He, G.-L.; Wu, C.-X.; Sommer, J.-U. Surface Instabilities of Monodisperse and Densely Grafted Polymer Brushes. *Macromolecules* **2008**, *41*, 5070.
(30) Egorov, S.; Romeis, D.; Sommer, J.-U. Surface Instabilities of Minority Chains in Dense Polymer Brushes: A Comparison of Density Functional Theory and Quasi-off-lattice Self-consistent Field Theory. *J. Chem. Phys.* **2012**, *137*, 064907.
(31) Milner, S. T.; Witten, T. A.; Cates, M. E. Effects of Polydispersity in the End-grafted Polymer Brush. *Macromolecules* **1989**, *22*, 853−861.
(32) Dan, N.; Tirell, M. Effect of Bimodal Molecular Weight Distribution on the Polymer Brush. *Macromolecules* **1993**, *26*, 6467−6473.
(33) Lai, P.-Y.; Zhulina, E. Structure of a Bidisperse Polymer Brush: Monte-Carlo Simulation and Self-Consistent Field Results. *Macromolecules* **1992**, *25*, 5201−5207.
(34) Goedel, W.; Luap, C.; Oeser, R.; Lang, P.; Braun, C.; Steitz, R. Stratification in Monolayers of a Bidisperse Melt Polymer Brush as Revealed by Neutron Reflectivity. *Macromolecules* **1999**, *32*, 7599−7609.
(35) Soga, K.; Zuckermann, M.; Hong, G. Binary Polymer Brush in a Solvent. *Macromolecules* **1996**, *29*, 1998−2005.
(36) Marko, J.; Witten, T. Phase Separation in a Grafted Polymer Layer. *Phys. Rev. Lett.* **1991**, *66*, 1541−1544.
(37) Milner, S. T.; Wang, Z.-G.; Witten, T. A. End-Confined Polymers: Corrections to the Newtonian Limit. *Macromolecules* **1989**, *22*, 489−490.
(38) Skvortsov, A.; Klushin, L.; Gorbunov, A. Long and Short Chains in a Polymeric Brush: A Conformational Transition. *Macromolecules* **1997**, *30*, 1818−1827.
(39) Skvortsov, A.; Gorbunov, A.; Leermakers, F.; Fleer, G. Long Minority Chains in a Polymer Brush: A First-Order Adsorption Transition. *Macromolecules* **1999**, *32*, 2004−2015.
(40) Witten, T.; Milner, S. Two-Component Grafted Polymer Layers. *Mater. Res. Soc. Symp. Proc.* **1990**, *177*, 37−45.
(41) Mueller, M. Phase Diagram of a Mixed Polymer Brush. *Phys. Rev. E: Stat., Nonlinear, Soft Matter Phys.* **2002**, *65*, 030802.
(42) Williams, D. Grafted Polymers in Bad Solvents: Octopus Surface Micelles. *J. Phys. II* **1993**, *3*, 1313−1318.
(43) Jentzsch, C.; Sommer, J.-U. Polymer Brushes in Explicit Poor Solvents Studied Using a New Variant of the Bond Fluctuation Model. *J. Chem. Phys.* **2014**, *141*, 104908.
(44) Fleer, G.; Cohen Stuart, M.; Scheutjens, J.; Cosgrove, T.; Vincent, B. *Polymers at Interfaces*, 1st ed.; Chapman Hall: London, 1993.
(45) Romeis, D.; Lang, M. Excluded Volume Effects in Polymer Brushes at Moderate Chain Stretching. *J. Chem. Phys.* **2014**, *141*, 104902.
(46) Mansoori, G. A.; Carnahan, N. F.; Starling, K. E.; Leland, T. W. Equilibrium Thermodynamic Properties of the Mixture of Hard Spheres. *J. Chem. Phys.* **1971**, *54*, 1523−1525.
(47) Boublik, T. Hard-Sphere Equation of State. *J. Chem. Phys.* **1970**, *53*, 471−472.
(48) Carnahan, N.; Starling, K. Equation of State for Nonattracting Rigid Spheres. *J. Chem. Phys.* **1969**, *51*, 635−636.
(49) de Vos, W. M.; Biesheuvel, P. M.; de Keizer, A.; Kleijn, J. M.; Cohen Stuart, M. A. Adsorption of Anionic Surfactants in a Nonionic Polymer Brush: Experiments, Comparison with Mean-Field Theory, and Implications for Brush-Particle Interaction. *Langmuir* **2009**, *25*, 9252−9261.
(50) Rubinstein, M.; Colby, R. *Polymer Physics*; Oxford University Press: Oxford, U.K., 2006.
(51) Klushin, L.; Skvortsov, A.; Polotsky, A.; Qi, S.; Schmid, F. Sharp and Fast: Sensors and Switches Based on Polymer Brushes with Adsorption-Active Minority Chains. *Phys. Rev. Lett.* **2014**, *113*, 068303.
(52) Skvortsov, A.; Klushin, L.; van Male, J.; Leermakers, F. First-order coil-to-flower transition of a polymer chain pinned near a stepwise external potential: Numerical, analytical, and scaling analysis. *J. Chem. Phys.* **2001**, *115*, 1586−1595.

DOI: 10.1021/am507959k
ACS Appl. Mater. Interfaces 2015, 7, 12496−12504